Author/s:
Debruin, DA;Murphy, J;Campelj, DG;Bagaric, R;Timpani, CA;Goodman, CA;Hanson, ED;Rybalka, E;Hayes, A

Title:
Combined orchiectomy and limb immobilization recapitulate early age‐related changes to skeletal muscle in mice

Date:
2024-01

Citation:
Debruin, D. A., Murphy, J., Campelj, D. G., Bagaric, R., Timpani, C. A., Goodman, C. A., Hanson, E. D., Rybalka, E. & Hayes, A. (2024). Combined orchiectomy and limb immobilization recapitulate early age‐related changes to skeletal muscle in mice. JCSM Communications, 7 (1), pp.40-54. https://doi.org/10.1002/rco2.90.

Persistent Link:
https://hdl.handle.net/11343/351161

ORIGINAL ARTICLE

JCSM Communications 2024; **7**: 40–54
Published online 16 April 2024 in Wiley Online Library (wileyonlinelibrary.com) **DOI:** 10.1002/rco2.90

Combined orchiectomy and limb immobilization recapitulate early age-related changes to skeletal muscle in mice

Danielle A. Debruin[1,2,3], Jasmaine Murphy[1], Dean G. Campelj[4], Ryan Bagaric[1,2], Cara A. Timpani[1,2,3], Craig A. Goodman[1,2,5], Erik D. Hanson[1,6], Emma Rybalka[1,2,3] & Alan Hayes[1,2,3]*

[1]*Institute for Health and Sport, Victoria University, Melbourne, Australia;* [2]*Australian Institute for Musculoskeletal Science (AIMSS), Sunshine Hospital, St Albans, Australia;* [3]*Department of Medicine - Western Health, Melbourne Medical School, The University of Melbourne, Melbourne, Australia;* [4]*Biology of Ageing Laboratory, Centenary Institute, Sydney, Australia;* [5]*Centre for Muscle Research (CMR), Department of Physiology, The University of Melbourne, Parkville, Australia;* [6]*Department of Exercise and Sport Science, University of North Carolina at Chapel Hill, Chapel Hill, NC, USA*

Abstract

Background Muscle mass and function decline in middle age, ultimately resulting in sarcopenia in the elderly and poor health outcomes, reducing quality of life. There is a lack of cost- and time-effective murine models that recapitulate the physiological changes associated with muscle mass decline to study possible interventions to delay sarcopenia. We aimed to evaluate the effectiveness of combining orchiectomy (ORC) surgery to simulate age-related androgen decline and hindlimb immobilization (IM) in inducing age-related skeletal muscle changes.

Methods Four-month-old male C57BL/6J mice (n = 10) were subjected to ORC, followed by IM (right hindlimb casting) for 14 days. Upon completion of the casting period, ex vivo muscle contractile function, histology, and various mitochondrial markers were assessed, and results were compared with age-matched controls (CON; n = 8) and middle-aged (MA; 12 ± 1 months, n = 9) animals.

Results IM combined with ORC induced a 30%–40% decrease in muscle mass across multiple hindlimb muscles ($P < 0.0001$), with the magnitude of muscle loss comparable with the MA group when corrected for body weight ($P < 0.0001$). In the IM limb of ORC mice, soleus muscle force significantly decreased when compared with the contralateral limb ($P < 0.05$) and aged-matched CON group ($P < 0.05$). The decrements in muscle force and mass present in the IM limb of ORC mice were accompanied by a 70% reduction in the expression of the muscle structural protein dystrophin and various mitochondrial markers, including cytochrome C (−55%), peroxisome proliferator-activated receptor gamma co-activator 1-beta (PGC1-β) (−49%), and cytochrome oxidase IV (COX-IV) (−73%) when compared with CON animals ($P < 0.001$). Lastly, our model also demonstrated specific fibre-type shifts in fast- and slow-twitch muscles, which mimicked changes in the MA group.

Conclusions Applying treatments during IM could target acute muscle atrophy in MA adults, while applying them following cast removal in a low-testosterone environment could represent a window for rehabilitation therapeutics.

Keywords Atrophy; Mouse model; Pre-clinical; Sarcopenia; Skeletal muscle; Strength

Received: 7 February 2023; Revised: 16 February 2024; Accepted: 20 February 2024
**Correspondence to: Alan Hayes, Institute for Health and Sport, Victoria University, Melbourne, VIC, Australia. Email: alan.hayes@vu.edu.au*

Introduction

Skeletal muscle has many functions essential for maintaining optimal health and well-being, highlighting that the preservation of its mass is critical for survival. This demands a balance between protein synthesis and degradation processes. Alterations in this balance can result in muscle growth or atrophy to the detriment of the organism. Typically, muscle atrophy occurs in response to conditions such as hypogravity,[1] muscle disuse,[2] and hyperinflammatory states associated with chronic disease, for example, diabetes.[3] In these conditions, addressing the underlying cause, such as re-loading muscle and tempering inflammation, reverses atrophy. However, muscle atrophy associated with increasing age, termed sarcopenia, cannot be reversed and leads to progressive loss of mass, function, and quality of life, as well as poor health outcomes.

Although a consensus on the clinical definition of sarcopenia is lacking, muscle changes appear to onset as early as middle age (~40 years). While the precise cause is unclear, these muscle changes coincide with the gradual decline of circulating androgens (e.g., testosterone), albeit muscle loss occurs at a considerably faster rate than androgen decline.[4] The putative role of testosterone in setting muscle size during adolescence and its anabolic properties are well established.[5,6] Mitochondrial dysfunction and changes to cytoskeletal composition are also hallmarks of aging muscle, although their cause is unclear.[6] Due to advancements in diagnostic tools (mostly imaging modalities),[7] sarcopenia is now more readily identified in the clinical setting, provoking a proportionate demand for effective interventions that slow its progression. Because sarcopenia cannot be reversed or prevented, early intervention during middle age provides the greatest scope for clinical efficacy. The hunt for suitable therapeutic targets within both muscle and other body systems and evaluating effective pharmaceutical, exercise, and nutritional interventions against them is currently an area of intense research focus.

Proof-of-concept and pre-clinical research frequently utilize murine models as a cost-effective tool to assess possible therapeutic interventions. Several mouse models of sarcopenia exist, including genetic mutants of accelerated aging. However, the gold standard model is the naturally aged mouse, in which muscles become sarcopenic within a systemic aging environment.[8,9] A significant drawback to using this model is the cost and time associated with housing mice for their 2- to 3-year lifespan to observe the impact of the experimental intervention on sarcopenia progression. An inducible mouse model that recapitulates sarcopenic changes to muscle in a cost-effective and timely manner is needed.

Herein, we have created a murine model of middle-age-onset sarcopenia in 4-month-old (~25 human years[10]) mice using two strategies. First, we induced androgen depletion via castration/orchiectomy (ORC) surgery to mimic endocrine-related muscle aging. Second, we induced atrophy via hindlimb immobilization (IM) using removable casting. We assessed our model against 12-month-old middle-aged (MA) mice that display early signs of the hallmarks of aging using function and histologic testing, including assessment of hallmarks of aging indicators, and showed good synergy.

Methods

Animals

This study was approved by the Victoria University Animal Ethics Committee (Project Codes 18/011 and 18/009) and performed in accordance with the Australian Code of Practice for the Care and Use of Animals for Scientific Purposes (National Health and Medical Research Council, Australia, 8th edition) and the ARRIVE guidelines.[11] C57BL/6J male mice (n = 16) at 4 months of age (equivalent to ~25 human years[10]) were obtained from the Animal Resources Centre (WA, Australia) and randomly assigned into age-matched control (CON; n = 8) or bilateral ORC (n = 8) groups. The right hindlimb of mice in the ORC group was subjected to IM with the contralateral left hindlimb uncasted (CNL). C57BL/6J male mice (n = 9) with an average age of 12 ± 1 month (MA; equivalent to 43–58 human years[12]) were used for comparative purposes.

Orchiectomy surgery

Under isoflurane anaesthesia (induction 4%, maintenance 2%), the scrotum was shaved, and both testes were extricated through a single midline incision along the scrotum. The vas deferens and testicular blood vessels were cauterized and returned to the scrotal sac with the epididymal fat. The scrotal incision was clamped, sutured (non-resorbable 4.0 thread), and sealed with wound glue (3M Vetbond™, Lyppard Australia Ltd.). The area was swabbed with povidone-iodine topical antiseptic and injected with 0.5% lignocaine and 0.2% bupivacaine for analgesia. Animals were recovered in a heated recovery box until fully conscious and then returned to their normal housing cages.

Immobilization protocol

Unilateral hindlimb IM was performed on all ORC mice 1 week after surgery, as described previously.[13,14] Briefly, animals were lightly anaesthetized, and the right hindlimb was immobilized by placing the limb through a cast (a 1.5-mL microtube and a paper clip). The foot was then secured in

total plantar extension and complete knee extension, placing the gastrocnemius, soleus, and plantaris muscles in a shortened position. The contralateral leg remained loose to allow for ambulation and was utilized as a control for the immobilized leg of each animal. To validate this as an internal control, our data demonstrated no significant differences in raw muscle mass (other than the plantaris) and no differences when corrected for body weight between the CON and CNL muscles from ORC mice (*Table 2*). At the end of the 14-day IM period, mice were anaesthetized with the casting material removed to allow for the collection of the hindlimb muscles. A subgroup of animals (n = 10) were immobilized for 2 weeks and used as a sham control to compare the effects of ORC on the muscle response to IM.

Ex vivo muscle contractile experiments

An *ex vivo* evaluation of muscle contractile properties was performed as described by us previously.[15] Briefly, excised extensor digitorum longus (EDL) and soleus muscles were placed into individual organ baths (Danish Myogenic Technology, Denmark) filled with Krebs–Henseleit Ringer's solution (118 mM of NaCl, 4.75 mM of KCl, 1.18 mM of $MgSO_4 7H_2O$, 1 mM of Na_2HPO_4, 2.5 mM of $CaCl_2H_2O$, 24 mM of $NaHCO_3$, and 11 mM of glucose). Each organ bath was bubbled with carbogen (5% CO_2/95% O_2) and maintained at 30°C and a pH of 7.4. The proximal end of the muscle was attached (via knotted surgical silk loops) to a previously calibrated force transducer, and the distal end was fixed to a micromanipulator with stimulating electrodes flanking the muscle belly. After optimal length was determined, absolute twitch and tetanic force production were established, followed by a force frequency relationship as described by us previously. Lastly, to investigate the fatigability of the muscles, both the EDL and soleus were stimulated intermittently. The EDL was stimulated once every 4 s for 350 ms at 100 Hz and the soleus once every 2 s at 80 Hz for 500 ms for a total of 3 min. Specific force production (force elicited per cross-sectional area) was also calculated according to Brooks and Faulkner.[16] Data were collected and analysed using LabChart Pro Version 8.0 software, customized for this experiment (AD Instruments, NZ).

Sample collection

As the ORC mice were to be directly compared with the MA animals to evaluate the effectiveness of the protocol, samples were taken immediately upon cast removal. The ORC mice were deeply anaesthetized via isoflurane; the cast was removed, and muscles of interest were surgically excised. Following excision of the EDL and soleus for contractile experiments, hindlimb muscles, including the tibialis anterior (TA), gastrocnemius, plantaris, and quadriceps, and other tissues were harvested, immediately weighed, and snapped frozen in liquid nitrogen for later analysis.

Quantification of circulating testosterone levels

To evaluate the effectiveness of bilateral castration to induce a decline in circulating testosterone, blood was collected from CON and ORC mice upon surgery day for cast removal. The MA mice did not have blood collected as these animals were part of a different study and there was insufficient blood remaining for analysis. Briefly, ~1 mL of blood was extracted from the femoral artery, placed on ice for 30 min to allow for clotting, and centrifuged at ×10 g for 5 min at 4°C. Following this, the supernatant was collected and stored at −80°C for later analysis. Samples were thawed, and testosterone levels were analysed using an enzyme-linked immunosorbent assay (ELISA) kit according to the manufacturer's instructions (Crystal Chem, IL, USA).

Histological staining and analysis

Following the completion of the contractile protocol, the EDL and soleus muscles were coated in an optimal cutting temperature (OCT) compound and snap frozen in liquid nitrogen-chilled isopentane (Sigma Aldrich, Australia). The embedded muscles were cryosectioned (12 μm), and a suite of stains were performed to quantify muscle atrophy [haematoxylin and eosin (H&E)], neutral lipid content [oil-red-o (ORO)], muscle phenotype (myosin ATPase), and mitochondrial capacity [succinate dehydrogenase (SDH)] as described previously[15] and analysed in blinded fashion.

Western blotting

As there is a lack of comparison in the literature between the changes seen in muscle integrity with aging and disuse, we characterized two membrane proteins of the dystrophin glycoprotein complex (DGC), dystrophin (1:300; Abcam #AB15277) and β-dystroglycan (1:500; Developmental Studies Hybridoma Bank #MANDAG2(7D11)), which play key roles in sarcolemma stability and integrity.[17] Additionally, we investigated mitochondrial markers [peroxisome proliferator-activated receptor gamma co-activator 1-beta (PGC1-β; 1:1000; Abcam #AB176328), cytochrome oxidase IV (COX-IV; 1:1000; Cell Signaling #4850), and cytochrome C (Cyt-C; 1:1000; Cell Signaling #11940)] to complement our histology data. The gastrocnemius was utilized as the muscle that best reflects human muscles due to its composition of both glycolytic and oxidative fibres. Further details regarding the western blotting protocol can be found in our recent publication.[15]

Statistics

Initially, a two-way analysis of variance (ANOVA) was performed with ORC and IM set as factors to compare the effects of combining both interventions using GraphPad Prism (Version 9.0). Thereafter, a one-way ANOVA was performed comparing the CON, MA, and IM muscles of ORC mice with a Tukey's multiple comparisons test where appropriate. A Student's *t*-test was conducted to determine between-limb effects within the ORC group. Alpha was set at 0.05.

Results

Orchiectomy decreased soleus force production in immobilized muscle

To establish the degree to which 3 weeks of ORC impacts muscle loss when combined with 2 weeks of IM, mice that were immobilized with and without ORC surgery (sham) were compared. As depicted in *Figure 1A*, mice were subjected to either sham or ORC surgery and allowed 7 days to recover before the application of an IM cast for 14 days. Following the IM period, casts were removed, and muscles from both IM and CNL limbs were analysed for muscle mass and contractile function. Overall, it was found that ORC did not impact endpoint body weight when compared with sham surgery (*Figure 1B*). IM decreased relative muscle mass of the EDL ($P < 0.0001$), soleus ($P < 0.0001$), TA ($P < 0.001$), plantaris ($P < 0.001$), and quadriceps ($P < 0.05$) when compared with CNL muscles in both sham and ORC mice (*Figure 1C–1G*). Interestingly, ORC further decreased soleus ($P < 0.01$) and plantaris ($P < 0.0001$) relative mass in both CNL and IM limbs when compared with sham animals. A post hoc interaction in the quadriceps showed that muscle mass increased in the CNL limb of ORC mice compared with sham ($P < 0.05$) but did not impact the IM limb in both groups.

Maximal contractile force production (absolute force) was assessed in the EDL and soleus muscles and corrected for cross-sectional area (specific force). In the EDL, ORC did not affect absolute or specific force output when compared with sham (*Figure 1H* and *1I*, respectively). However, IM decreased absolute force production in both sham and ORC animals ($P < 0.01$). In the soleus, absolute ($P < 0.05$; *Figure 1J*) and specific force ($P < 0.001$; *Figure 1K*) decreased in both the CNL and IM limbs of ORC mice when compared with sham animals, demonstrating an amplified, detrimental effect of bilateral ORC on slow-twitch force production. IM decreased soleus absolute ($P < 0.0001$) and specific force ($P < 0.0001$) profoundly in both the sham and ORC groups.

When evaluating the effect of the combined intervention on muscle fatigability, our data showed differing responses in the EDL and soleus muscles. In the EDL, both CNL and IM limbs of ORC mice were less fatigable when compared with both limbs of the sham animals ($P < 0.0001$; *Figure 2A*). However, the absolute force produced during the 3 min of repeated contractions decreased in the CNL limb of ORC mice but not on the IM side when compared with the sham animals ($P < 0.0001$; *Figure 2B*). Conversely, the soleus muscles of ORC mice were less fatigable compared with sham in both CNL ($P < 0.001$) and IM limbs ($P < 0.0001$; *Figure 2C*). However, the rate of force decline in both CNL and IM muscles of sham mice was comparable, demonstrating no effect of IM on soleus fatiguability in these animals. Not surprisingly, the IM soleus of both sham and ORC mice produced less force during the fatigue protocol when compared with all groups ($P < 0.0001$; *Figure 2D*). Lastly, force production tended to decrease in both CNL and IM limbs of ORC mice ($P = 0.08$, $P = 0.09$, respectively). Overall, it appears that bilateral ORC exacerbates the decrease in absolute and specific force production of IM muscle, with marked changes observed in the soleus when compared with un-orchiectomized mice.

Immobilized muscle mass of orchiectomized mice is comparable with that of middle-aged mice when corrected for body weight

With considerable differences in relative muscle mass of the soleus and plantaris between sham and ORC mice as well as exaggerated functional deficits in the soleus with ORC surgery, the data presented herein for the ORC group will be compared with MA (12-month-old) mice, where similar levels of testosterone are expected, and age-matched controls (4 months). As anticipated, bilateral ORC significantly decreased testosterone levels by more than 50% when compared with the CON group ($P < 0.05$, *Table 1*). Although testosterone measures could not be made on the MA animals, the changes observed in the ORC animals are similar to the age-related changes previously reported in male mice at 12 months of age.[18] The MA mice were significantly heavier than both the CON ($P < 0.05$) and ORC animals ($P < 0.001$; *Table 2*), with the same pattern observed in epididymal fat content ($P < 0.0001$). Muscle fibre atrophy was also present in both the EDL and soleus, with a marked reduction in fibre cross-sectional area found in the IM limb of ORC mice when compared with CONs and the CNL side ($P < 0.01$; *Figure S3*). Given the large disparity in body weights between the groups, all hindlimb muscles harvested were weighed and normalized to body weight (mg/g; *Table 2*). Of the raw muscle masses measured, all were lower in the IM limb of ORC mice when compared with CON and MA. All normalized muscle masses were lower in MA mice compared with the CON animals ($P < 0.05$), and all IM muscles of ORC mice were significantly lower compared with the CNL side ($P < 0.05$). Importantly, the IM muscle masses were comparable with

Figure 1 Evaluation of relative muscle mass and contractile function of immobilized muscle with and without orchiectomy (ORC). All mice were subject to either sham or ORC surgery 1 week prior to immobilization (IM) of the right limb. Following 2 weeks of IM, mice were killed, and both contralateral (CNL) and IM limbs were assessed for muscle mass and ex vivo contractile function. (A) Schematic of the experimental group for sham and ORC comparison. (B) Endpoint body weight. Muscle mass of the extensor digitorum longus (EDL; C), soleus (SOL; D), plantaris (PLT; E), tibialis anterior (TA; F), and quadriceps (QUAD; G) corrected for body weight (relative mass; mg/g). EDL absolute tetanic force production (H) and corrected for cross-sectional area (specific force; I). SOL absolute (J) and specific (K) force production. Symbols indicate $^{\wedge}P < 0.05$, $^{\wedge\wedge}P < 0.01$, $^{\wedge\wedge\wedge}P < 0.001$, $^{\wedge\wedge\wedge\wedge}P < 0.0001$ = immobilization main effect; $^{\dagger}P < 0.05$, $^{\dagger\dagger}P < 0.01$, $^{\dagger\dagger\dagger\dagger}P < 0.0001$ = orchiectomy main effect. Post hoc interaction: $^{\gamma\gamma}P < 0.01$ = orchiectomy effect; $^{\delta}P < 0.05$, $^{\delta\delta\delta\delta}P < 0.0001$ = immobilization effect. n = 8–10 per group.

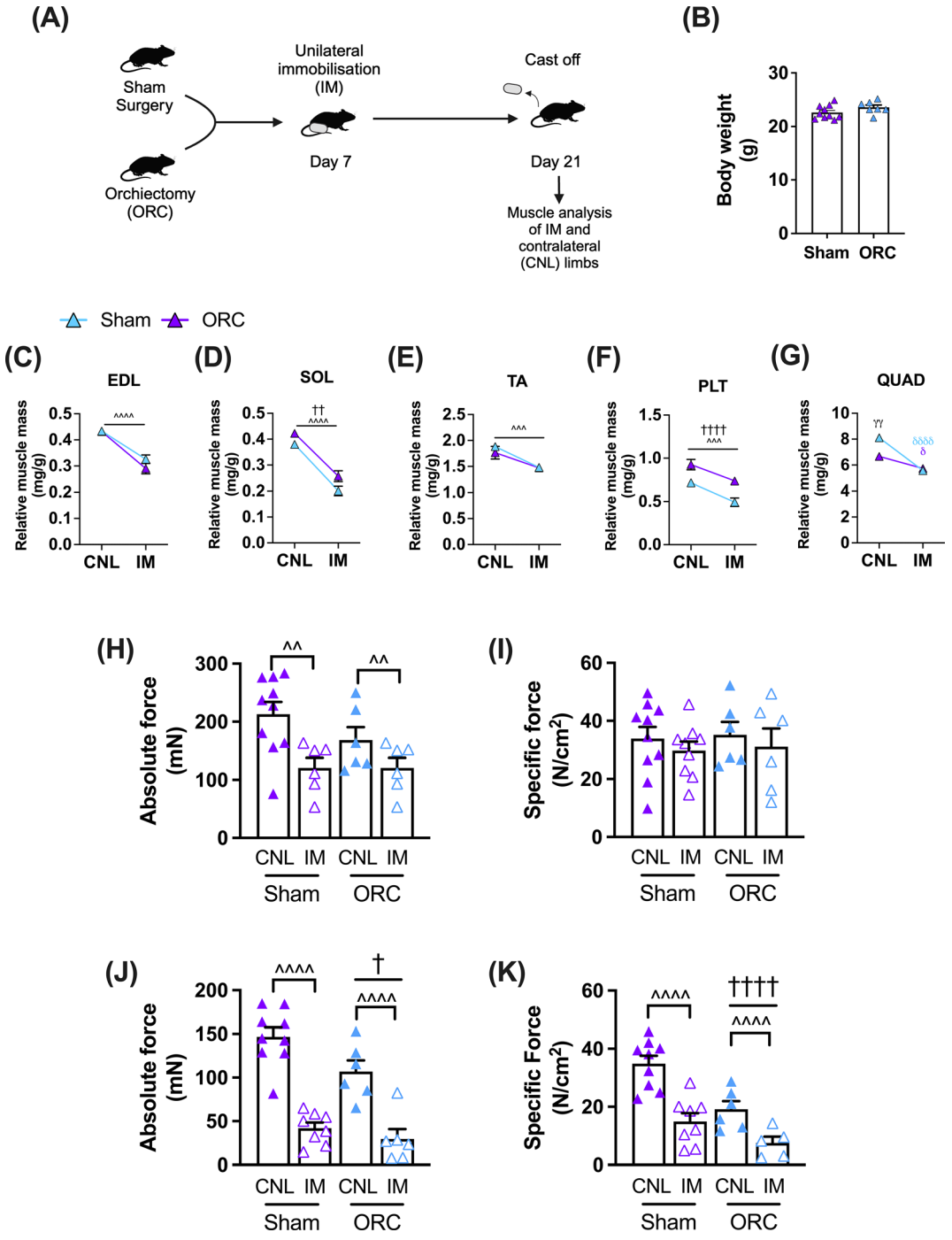

Figure 2 Ex vivo assessment of muscle fatigue extensor digitorum longus (EDL) and soleus muscles of sham and orchiectomized (ORC) mice subjected to immobilization. All mice were subject to either sham or orchiectomy (ORC) surgery 1 week prior to immobilization (IM) of the right limb. Following 2 weeks of IM, mice were killed, and both contralateral (CNL) and IM limbs were assessed for muscle fatigue. Muscles received constant stimulation once every 4 s (100 Hz, 350 ms duration) for the EDL and once every 2 s for the soleus (80 Hz, 500 ms duration) for 3 min. Muscle fatiguability of the EDL expressed as the percentage of initial contraction (A) and absolute force (B). Soleus muscle fatigability expressed as the percentage of initial contraction (C) and absolute force (D). n = 8–10 per group. Symbols indicate ^^$P < 0.01$, ^^^^$P < 0.0001$ = immobilization main effect; $^{††}P < 0.01$, $^{††††}P < 0.0001$ = orchiectomy main effect.

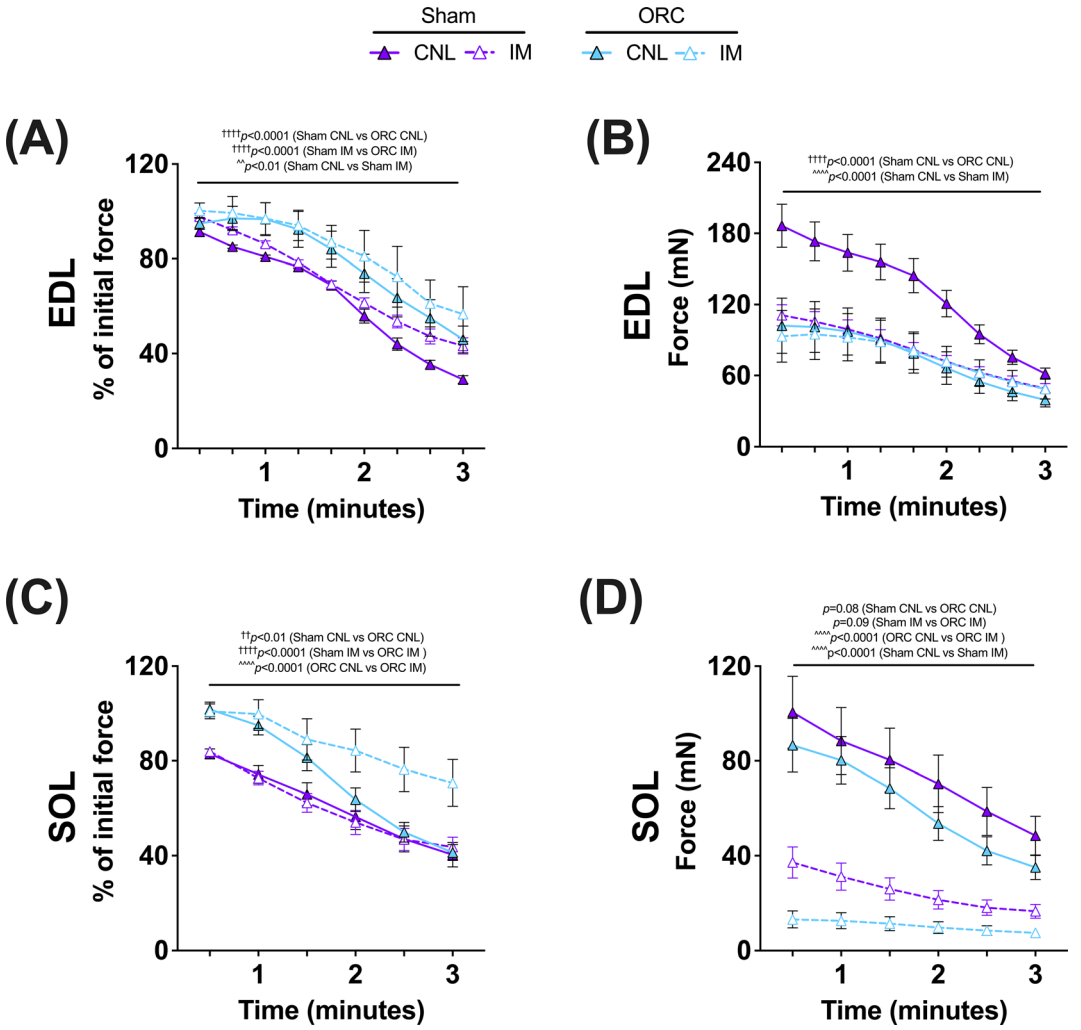

Table 1 Endpoint serum testosterone levels

	Testosterone level (ng/mL)	*P*-value (Student's *t*-test)
CON	4.1 ± 0.6	0.028
ORC	1.4 ± 0.6	
12-month-old male C57BL/6J mice (according to Davidyan et al.[18])	1.0	

Abbreviations: CON, control; ORC, orchiectomy.

those of the MA mice. We saw no evidence of compensatory hypertrophy in the CNL hindlimb of ORC animals, as absolute and normalized muscle masses were comparable with CON, except for the absolute mass of the plantaris, where there was a slight decrease in the CNL side ($P < 0.05$; *Table S1*).

Changes to contractile properties and fibre type of the soleus are similar between the middle-aged and immobilized muscles of orchiectomized mice

The soleus muscle of ORC animals, which was shortened during the IM phase (*Figure 3A*), was extracted upon cast removal, tested for ex vivo contractile properties, and

DOI: 10.1002/rco2.90

Table 2 Body mass and morphometric analysis of various hindlimb muscles

	Units	CON (n = 8)	MA (n = 9)	ORC (n = 8)	
Body weight	g	27.66 ± 0.60	39.78 ± 2.19****		23.60 ± 0.44$^{\#\#\#\#}$
Epi fat	mg/g	0.013 ± 0.001	0.038 ± 0.002****		0.005 ± 0.001*$^{\#\#\#\#}$
				CNL	**IM**
EDL	mg/g	0.44 ± 0.01	0.33 ± 0.03***	0.43 ± 0.01	0.32 ± 0.02****^ ^
SOL		0.32 ± 0.01	0.29 ± 0.02**	0.36 ± 0.01	0.20 ± 0.01****$^{\#\#}$^ ^ ^ ^
PLT		0.69 ± 0.03	0.56 ± 0.06*	0.71 ± 0.03	0.49 ± 0.05*^ ^
GAST		4.79 ± 0.09	3.7 ± 0.26***	4.90 ± 0.7	3.64 ± 0.16****^ ^ ^ ^
TA		1.80 ± 0.05	1.29 ± 0.08****	1.88 ± 0.05	1.48 ± 0.07****^ ^
QUAD		7.9 ± 0.17	4.57 ± 0.39**	8.1 ± 0.24	5.57 ± 0.26**^ ^

Note: The right hindlimb of the ORC animals was immobilized (IM) and the contralateral left limb uncasted (CNL).
Abbreviations: CON, control; EDL, extensor digitorum longus; Epi, epididymal; GAST, gastrocnemius; MA, middle-aged; ORC, orchiectomy; PLT, plantaris; QUAD, quadriceps; SOL, soleus; TA, tibialis anterior.
*$P < 0.05$.
**$P < 0.01$.
***$P < 0.001$.
****$P < 0.0001$—different from CON.
$^{\#\#}P < 0.01$.
$^{\#\#\#\#}P < 0.0001$—different from MA.
^ ^$P < 0.01$.
^ ^ ^ ^$P < 0.0001$—different from CNL limb.

compared with all other groups. There were no significant differences in absolute twitch, tetanic, or specific force production of soleus muscles between the CON and MA animals (*Figure 3B–3D*). Absolute twitch force production in the soleus was lower in the IM muscle of ORC mice compared with all other groups ($P < 0.05$; *Figure 3B*), with the same differences seen with absolute tetanic force ($P < 0.05$; *Figure 3C*) except when compared with MA. Specific force production was also lower in the IM soleus muscle compared with CNL in ORC mice ($P < 0.05$; *Figure 3D*). As an indication of calcium handling abilities, a force–frequency relationship was determined by stimulating the muscle at increasing frequencies, with absolute force recorded and displayed as a percentage of peak tetanic force (*Figure 3E*). A leftward shift was found in the IM muscle compared with CON ($P = 0.055$) and MA ($P < 0.001$). The IM muscle of ORC mice was significantly less fatigable compared with CON ($P < 0.0001$) and MA ($P < 0.0001$) animals, as well as the CNL limb ($P < 0.001$; *Figure 3F*). Conversely, the MA animals were more fatigable than the CON group ($P < 0.0001$). Muscle fatigue is caused by both the metabolic capacity of the muscle and the absolute force produced. To determine whether reduced muscle fatigability of the ORC muscles was due to less force produced across the fatigue protocol, we assessed raw absolute force production across the fatigue period, as less force output may explain why the muscles were relatively resistant to fatigue (*Figure 3G*). Despite only a 20% drop in initial force in the soleus of IM muscle during the fatigue protocol, the very low absolute forces to begin with meant that across the 3-min period, the force elicited was significantly lower compared with CON ($P < 0.0001$), MA ($P < 0.0001$), and CNL ($P < 0.001$) muscles. To evaluate oxidative capacity, SDH staining was performed, and intensity was expressed as a percentage of the total area analysed (*Figure 3H* and *3L*). Only the IM soleus of ORC mice was found to be different, with a lower oxidative capacity when compared with the MA group ($P < 0.05$). The neutral lipid content of the soleus was also determined via ORO staining, with no differences found across all groups (*Figure 3I* and *3L*). To elucidate if muscle fibre-type changes were responsible for the impaired contractile function observed in the IM muscles of ORC mice, we performed myosin ATPase staining in both the soleus (*Figure 3J–3L*) and EDL (*Figure 4J–4L*). In the soleus, all fibre types analysed decreased in size in the IM limb of ORC mice compared with CON and MA animals ($P < 0.05$; *Figure 3J*). Regarding fibre-type composition (*Figure 3K*), the percentage of type I fibres decreased in the IM soleus when compared with CON ($P < 0.01$) and the CNL side ($P < 0.01$). Similar decreases in the amount of type I fibres were also found in the MA group when compared with CON ($P < 0.01$). Contrary to the decrease found in the amount of type I fibres, the quantity of type IIA fibres increased in both MA ($P < 0.05$) and IM muscles of ORC animals ($P < 0.0001$) when compared with CON. In the ORC animals, the IM soleus muscle also contained a greater percentage of type IIA fibres compared with the CNL side ($P < 0.0001$). Lastly, it was only the IM soleus that contained fewer type IIX fibres compared with the CON and CNL limbs of ORC mice ($P < 0.05$).

Fibre-type profiles, but not contractile properties, are altered in the immobilized extensor digitorum longus muscle of orchiectomized mice

Ex vivo contractile analysis was conducted in the fast-twitch EDL muscle (*Figure 4A*) in all groups. There was no differ-

Figure 3 Functional and histological characterization of the soleus (SOL) muscle of control (CON), middle-aged (MA), and immobilized orchiectomized (ORC) mice. The right hindlimb of the ORC animals was immobilized (IM) and the contralateral left limb uncasted (CNL). (A) Anatomical positioning of the SOL demonstrating the shortening of the muscle during the immobilization phase of the ORC mice. Ex vivo contractile analysis outcomes including peak twitch (B), absolute (C), and specific force (D) with the force–frequency relationship demonstrated in panel (E). Muscle fatigability was assessed across a 3-min protocol, with data presented as the percentage initial force (F) and absolute force (G). Oxidative capacity quantified via succinate dehydrogenase (SDH) (H) and neutral lipid content via oil-red-o (ORO) staining (I). Fibre-type isoforms were quantified via ATPase with the average fibre area (J) and percentage of total fibres (K) analysed. Representative images of the ORO, ATPase, and SDH stains displayed in panel (L). Symbols indicate $*P < 0.05$, $**P < 0.01$, $***P < 0.001$, $****P < 0.0001$—different from CON; $^{\#}P < 0.05$—different from MA; $\wedge P < 0.05$, $\wedge\wedge P < 0.01$, $\wedge\wedge\wedge\wedge P < 0.0001$—IM different from CNL. Scale bar = 100 μm. n = 4–6 per group.

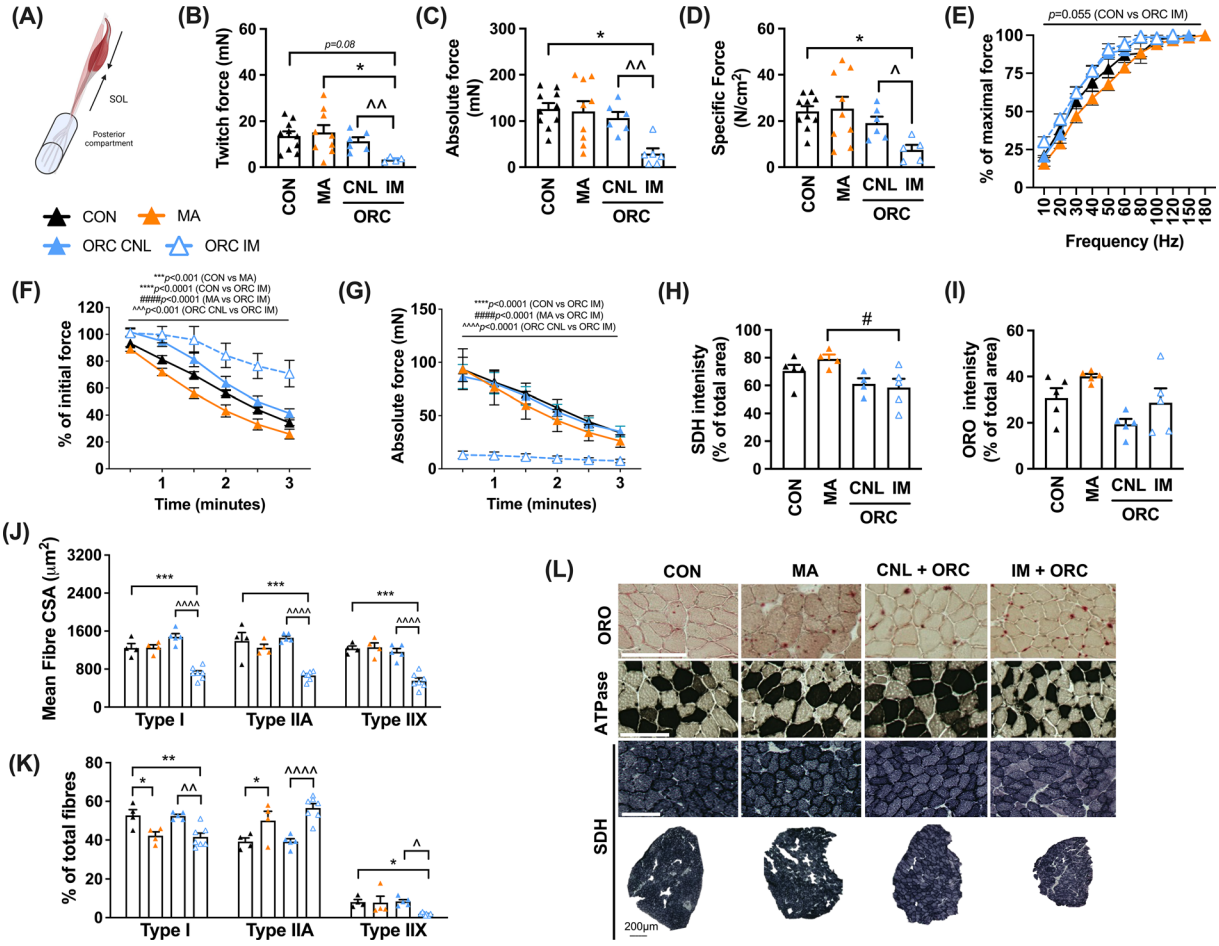

ence in EDL absolute twitch and tetanic force production of the MA mice when compared with the CON and ORC groups, with only the IM muscle eliciting significantly lower tetanic forces when compared with the CON animals ($P < 0.05$; *Figure 4C*). However, there was a strong trend for the MA EDL muscles to produce less specific force compared with CON animals ($P = 0.07$; *Figure 4D*). Even though the IM EDL of ORC mice was smaller, the specific force was not significantly different from that of the CON animals or the CNL side The force output of EDL muscles from the CNL limb of ORC mice was comparable with that of CON animals, demonstrating no compensatory effects on strength from IM (*Figure 4B–4D*). A rightward shift in the force–frequency relationship of the MA EDL was observed, suggesting decreased sensitivity of the muscles to calcium or a faster phenotype (*Figure 4E*). The IM EDL muscles of ORC mice were less fatigable than those from the CON and MA animals across the 3 min of induced fatigue ($P < 0.0001$; *Figure 4F*). Like the soleus, the fatigability of the MA EDL increased when compared with CON ($P < 0.05$). As we did for the soleus, we assessed absolute force production across the fatigue protocol and found that the force output of the IM EDL muscles of the ORC mice was lower than CON ($P < 0.01$) across the whole fatigue protocol (*Figure 4G*). However, EDL muscles from MA animals elicited significantly lower raw absolute forces compared with CON ($P < 0.0001$) and IM muscles

Figure 4 Functional and histological characterization of the extensor digitorum longus (EDL) muscle of control (CON), middle-aged (MA), and immobilized orchiectomized (ORC) mice. The right hindlimb of the ORC animals was immobilized (IM) and the contralateral left limb uncasted (CNL). (A) Anatomical positioning of the EDL demonstrating the lengthening of the muscle during the immobilization phase of the ORC mice. Ex vivo contractile analysis outcomes including peak twitch (B), absolute (C), and specific force (D) with the force–frequency relationship demonstrated in panel (E). Muscle fatigability was assessed across a 3-min protocol, with data presented as the percentage initial force (F) and absolute force (G). Oxidative capacity quantified via succinate dehydrogenase (SDH) (H) and neutral lipid content via oil-red-o (ORO) staining (I). Fibre-type isoforms were quantified via ATPase with average fibre area (J) and percentage of total fibres (K) analysed. Representative images of the ORO, ATPase, and SDH stains displayed in panel (L). Symbols indicate *$P < 0.05$, **$P < 0.01$, ***$P < 0.001$, ****$P < 0.0001$—different from CON; ^$P < 0.05$, ^^$P < 0.01$, ^^^$P < 0.001$, ^^^^$P < 0.0001$—IM different from CNL. Scale bar = 100 μm. n = 4–6 per group.

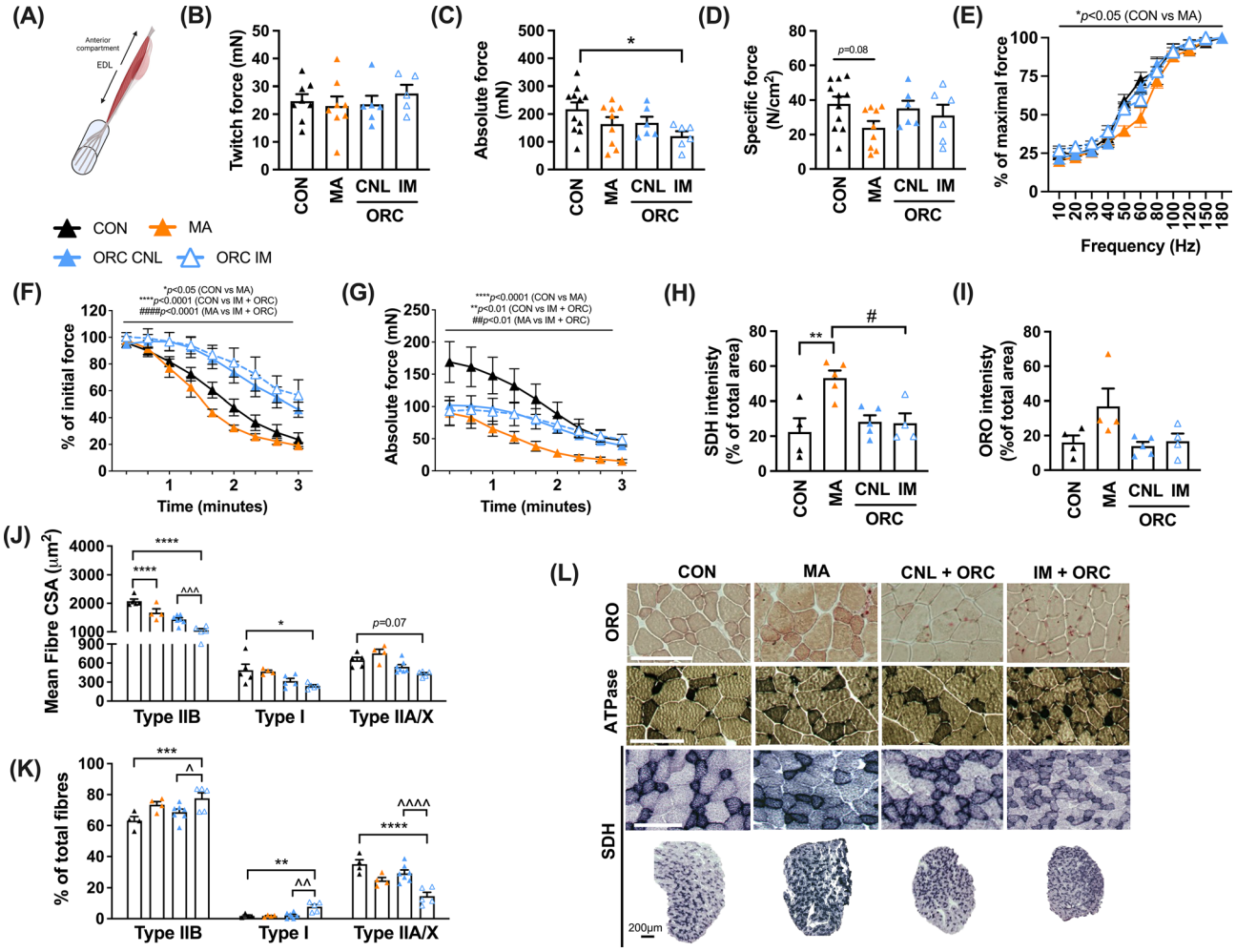

($P < 0.01$). SDH intensity increased in MA animals compared with both CON ($P < 0.01$) and IM muscles of ORC mice ($P < 0.05$; *Figure 4H* and *4L*). Similar to the soleus, ORO staining did not change between groups (*Figure 4I* and *4L*). Interestingly, there was a stark increase in the number of type I fibres in the IM muscle of ORC mice compared with CON, MA, and CNL muscles ($P < 0.01$; *Figure 4J* and *4L*). An increase in the proportion of type IIB fibres was also observed in the IM EDL muscle of ORC mice compared with the CON ($P < 0.001$) and the CNL side ($P < 0.05$). Unsurprisingly, the proportion of type IIA/X fibres in the EDL was drastically reduced in the IM muscle of ORC mice compared with the CON ($P < 0.001$), MA ($P < 0.05$), and CNL side ($P < 0.0001$). Consistent with our H&E data (*Figure S3*), the cross-sectional area of all fibre types in the EDL was significantly smaller in the IM muscles of ORC mice compared with the CON and MA muscles ($P < 0.05$; *Figure 4K*). Compared with the CON muscles, changes in fibre-type proportions occurred in the MA EDL muscles, although these differences were not as stark. There was a higher percentage of type I and IIB fibres in the IM EDL of ORC mice when compared with CON and CNL sides ($P < 0.05$), while the proportions of type IIA/X fibres

were significantly reduced ($P < 0.05$). Type IIX fibres are hybrids that manifest both type I and type IIB characteristics, making them more adaptable to environmental cues; thus, their loss in the MA group and the IM muscle of ORC mice suggests reduced adaptability. However, unlike the IM muscles, the alteration in fibre-type proportions in the MA muscles was counteracted by concomitant oppositional changes in fibre area. As such, while the type IIB fibre cross-sectional area decreased in size ($P < 0.0001$), the type IIA/X fibre area increased compared with the CON EDL muscles ($P < 0.05$).

Dystrophin expression decreases in immobilized muscle

The DGC in skeletal muscle plays an essential role in supporting force transmission by enabling stable interactions between the sarcolemma and the cytoskeleton. Interestingly, we found that the expression of dystrophin decreased significantly in response to IM when compared with CON animals ($P < 0.001$) and trended to decrease in the MA group ($P = 0.07$; *Figure 5A*). The IM muscle of ORC mice also had lower dystrophin expression compared with the MA animals

Figure 5 Characterization of dystrophin, β-dystroglycan, and various mitochondrial-related proteins from the gastrocnemius muscle of control (CON), middle-aged (MA), and orchiectomized-immobilized (ORC) mice. The right hindlimb of the ORC animals was immobilized (IM) and the contralateral left limb uncasted (CNL). Western blot analysis of dystrophin glycoprotein complex proteins dystrophin (A) and β-dystroglycan (β-DG; B). Succinate dehydrogenase (SDH) staining of the tibialis anterior muscle (C) with representative images in sub-panel (Ci). Mitochondrial-associated proteins, peroxisome proliferator-activated receptor gamma co-activator 1-beta (PGC1-β; D), cytochrome oxidase IV (COX-IV; E), and cytochrome C (Cyt-C; F) were also quantified via western blot. AMP-activated protein kinase (AMPK) protein expression was determined in its phosphorylated (pAMPK; G) and total (H) forms. The ratio of phosphorylated to total AMPK was calculated and presented in panel (I). Symbols indicate $*P < 0.05$, $**P < 0.01$, $***P < 0.001$—different from CON; $^{\#}P < 0.05$, $^{\#\#}P < 0.01$—different from MA; $\wedge P < 0.05$, $\wedge\wedge P < 0.01$—IM + ORC different from CNL + ORC. Scale bar = 100 μm. n = 4–6 per group. Western blot representative images cropped to remove lane containing sample unrelated to this study. To view full-length images of western blot gel, gel layout, and protein loading, refer to *Figure S4*.

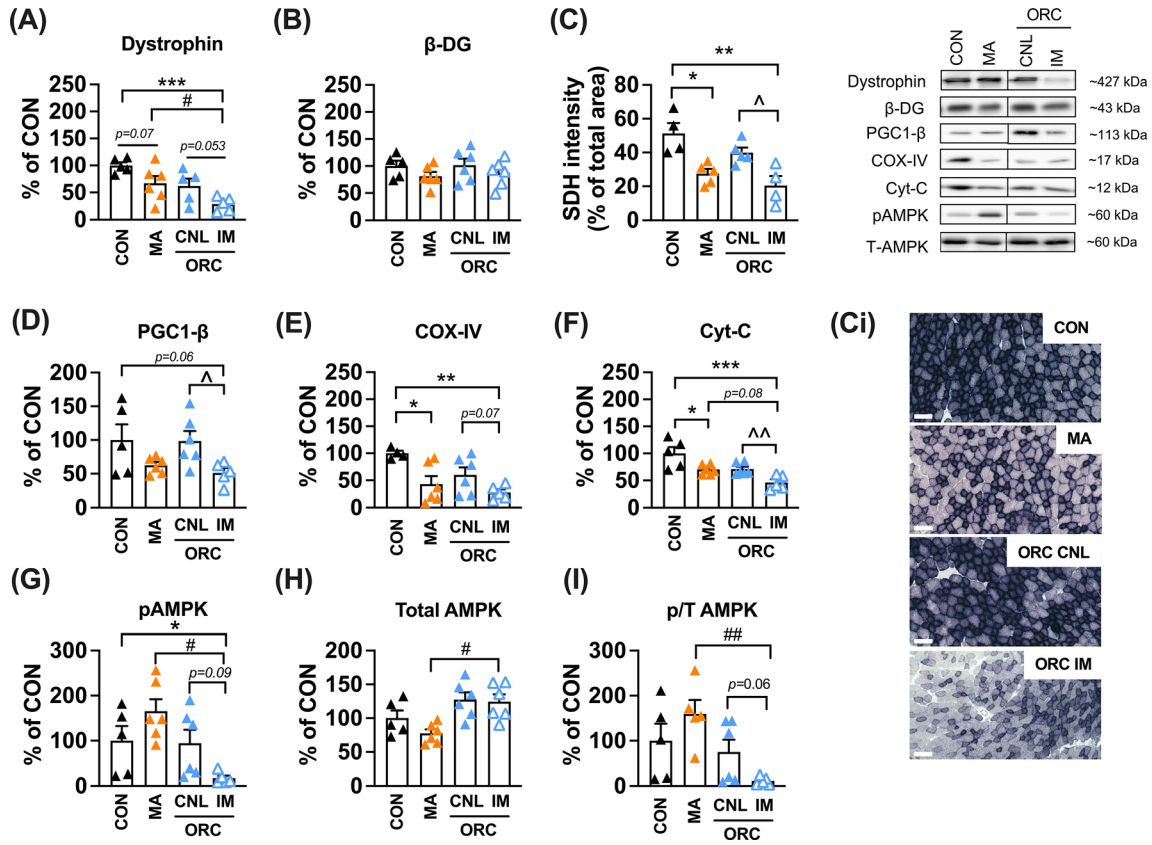

DOI: 10.1002/rco2.90

($P < 0.05$). There were no changes in β-dystroglycan expression between any of the groups (*Figure 5B*).

Decreased expression of mitochondrial proteins that control oxidative metabolism is consistent between middle-aged muscle and muscle subjected to the combination of immobilization and orchiectomy

To further characterize the model, mitochondrial markers were examined in MA and ORC animals, with specific mitochondrial proteins associated with oxidative metabolism investigated in the gastrocnemius. Oxidative metabolism is negatively impacted by aging and is a key feature of sarcopenic muscle.[19] With intriguing evidence demonstrating a link between membrane proteins and the mitochondria,[20] various mitochondrial-related proteins were subsequently investigated in the gastrocnemius via western blot. In addition, SDH staining was also performed on the TA muscle and expressed as a percentage of the total area analysed (*Figure 5C*). It was found that both SDH intensity decreased in both MA ($P < 0.05$) and IM muscles of ORC mice ($P < 0.01$) when compared with CON, with the level detected in the IM limb also lower than the CNL side ($P < 0.01$). The expression of PGC1-β, a key marker of mitobiogenic transcriptional activity, was compared between groups (*Figure 5D*). PGC1-β protein expression significantly decreased in the IM muscles of ORC mice compared with CON and the CNL limb ($P < 0.05$), with no significant change observed in the MA group. Two other mitochondrial proteins associated with oxidative metabolism, COX-IV and Cyt-C, were also quantified (*Figure 5E* and *5F*, respectively). The expression of COX-IV decreased in both the MA ($P < 0.05$) and IM muscles of ORC mice ($P < 0.01$) when compared with CON animals, with a trend for a decrease between CNL and IM limbs ($P = 0.07$). Similarly, Cyt-C expression decreased in the MA ($P < 0.05$) and IM muscles of ORC mice ($P < 0.001$) when compared with CON. In addition, Cyt-C levels tended to decrease in the IM limb of ORC animals when compared with the MA group ($P = 0.08$) but were significantly lower than levels found on the CNL side ($P < 0.01$).

The phosphorylation of AMP-activated protein kinase (AMPK) (T172), a protein responsible for sensing nutrient/energy deficits, decreased significantly in the IM muscle of ORC animals compared with CON ($P < 0.01$; *Figure 5G*). There was also a strong trend for phosphorylated AMPK to decrease in the MA group and the IM muscle ($P = 0.07$; *Figure 5G*). Total AMPK was significantly higher in IM muscle compared with MA ($P < 0.05$; *Figure 5H*), but the phosphorylated to total AMPK ratio was significantly lower than the MA group ($P < 0.01$; *Figure 5I*). However, there were no significant differences observed between the CON and MA groups.

Discussion

The aim of the study was to evaluate the changes seen in skeletal muscle in a rapidly inducible murine model of middle-age-onset sarcopenia. Here, we present a novel mouse model that recapitulates various changes to skeletal muscle consistent with middle age and displays several hallmarks of aging. In particular, this period represents a symptomatically detectable window for optimal therapeutic targeting to delay sarcopenia progression.

For many years, rodent models of sarcopenia were generated using techniques that either induced global or localized muscle atrophy in the hindlimb by genetic, denervation techniques, or pharmacological modification. In this study, to mimic the combined physiological changes seen with aging and inactivity, our model was created using both ORC surgery (to reduce testosterone as seen with aging in men) and hindlimb casting (to drive a rapid decline in muscle mass). We successfully induced a 60% reduction in circulating testosterone, consistent with reductions in aging humans and other castration studies.[18,21,22] To test the robustness of our model, functional, histological, and cytoskeletal characteristics of skeletal muscle were compared with those of MA mice. The complexities surrounding the pathogenesis of sarcopenia and associated muscle changes are only now being characterized by key alterations, including global reduction of muscle mass,[3] loss of muscle strength,[23] increased fatigue,[24] and intramuscular adipose tissue.[25] Recently, as stated in an expert opinion piece by Lynch,[6] the molecular underpinnings of these changes may be related to, but not limited to, the DGC, mitochondria, and hormone levels. Alterations of these factors featured in MA as potentially early indications of aging, and importantly in our ORC groups, demonstrating that the model reproduces changes seen in middle age as sarcopenia onsets. For example, MA mice had a lower muscle mass corrected for body weight and signs of poor muscle quality (as demonstrated by decreased specific force, particularly in the EDL), compared with 4-month-old CON mice. It was also evident that the MA EDL was weaker during the fatigue protocol, perhaps demonstrating early signs of mitochondrial dysfunction characteristic of all aged cells, including muscle fibres. Indeed, multiple studies in humans and rodents have shown that with age, mitochondrial integrity and function are compromised, which impacts physical performance.[26] Key changes include reduced energy production,[19] increased oxidative stress,[27] and impaired intracellular calcium regulation.[28] Mitochondrial integrity and functional decline are observed in mice from as early as 10–14 months preceding the onset of detectable sarcopenia[29] and may be central to the progressive loss of contractile performance and muscle mass. Our data suggest that a reduction of dystrophin protein is also involved. Loss of dystrophin protein is intimately linked to mitochon-

drial dysfunction in dystrophin-deficient mouse models, cancer cachexia, and human Duchenne muscular dystrophy (DMD) patients,[30] as well as drug-induced myopathy in mice.[31] To our knowledge, we are the first to demonstrate significantly reduced dystrophin protein expression in response to hindlimb IM with androgen depletion. Furthermore, we demonstrated a trend for dystrophin loss in MA animals, which supports previous findings.[32] Taken together, there is an associated link between the loss of dystrophin, increased fatigue, and decreased mitochondrial markers in the ORC model (and potentially during MA, signifying initial changes towards sarcopenia); however, further work is required to fully elucidate said relationship.

Observational studies have demonstrated an annual decline in muscle mass of 1% from the age of 40, equating to a loss of approximately 30%–40% by age 70.[33] The age of the MA mice used in this study was equivalent to 43–58 human years[12]; thus, we expected and observed only moderate declines in muscle mass. These changes are more representative of middle age, a time between healthy adult function and clinically diagnosable sarcopenia, during which a plethora of muscle changes occur, albeit at different rates, meaning that the MA period is appropriate to investigate preventative strategies for sarcopenia. Given that early functional changes in MA individuals may be too subtle to be readily detected in the clinic, the application of preventative strategies that preserve muscle mass and strength, such as regular resistance-based exercise, nutrition, or pharmacological intervention, is needed to avoid the onset of severe deterioration.[34] Longer casting periods could be used to increase severity, providing different starting points to test treatments against muscle wasting in a low-testosterone environment, as happens with older males. As such, we aimed to evaluate the extent to which our model compared to, or even exceeded, MA changes. Fourteen days of hindlimb IM in our model induced a 20%–30% loss in muscle mass, which was comparable with MA mice, taking into consideration differences in body weight (*Table 2*). The decrease in muscle mass seen in the ORC model is similar to that observed with aging—a 20% loss of muscle mass typically seen across a 15- to 20-year period.[7,33] With respect to muscle force production, there was a marked decrease in the slow-twitch soleus muscle of our model, which was far greater than in MA mice. Oxidative muscles, such as the soleus, are more impacted by unloading than fast-twitch muscles.[35] This is a key difference observed between the immobilized muscle combined with ORC and the MA animals and to aging in general, in which there is preferential atrophy of fast-twitch fibres and a slowing of the muscles.[36] In addition to this, muscles fixed in the shortened position during IM (i.e., the soleus in our study) atrophy to a greater extent than muscles that are lengthened.[37,38] Thus, it is possible to modify the hindlimb position to manipulate the loss in specific muscles in our model, which can be advantageous in designing studies where muscle phenotypic responses are a key focus.

Mitochondria have recently been implicated in many physiological processes associated with the maintenance of muscle mass and contractile performance.[39] In addition to this, the cross-talk between mitochondria and pathways involved in redox responses and inflammation is only beginning to be defined in muscle.[27,40–42] Many studies have demonstrated declines in mitochondrial density and function with aging in an array of tissues, including skeletal muscle.[27,41–43] We used SDH staining, which is used to quantify the abundance and activity of SDH enzymes comprising mitochondrial complex II. Although we observed increased fatigue of the EDL and soleus of MA compared with CON muscles (*Figure 3*), SDH activity increased. It was presumed that fatigue susceptibility could be explained by lower oxidative capacity, but the changes may in fact be more complex than that. As mitochondrial DNA (mtDNA) mutations accumulate through the lifespan, electron transport chain function (particularly of complexes I and IV) is severely compromised, and complex II compensates through increasing activity, albeit insufficiently.[43–45] Although these age-related changes were observed in MA mice, it is important to note that we did not observe the same changes in our ORC model consistent with the biological age of the mice (i.e., 4 months). The immobilized EDL of ORC mice was comparatively fatigue resistant relative to the CNL side and what was found in the CON group (which has been shown in previous studies[46]), but soleus was severely impacted with force output so low that muscle fatigue could not be properly induced with the use of our ex vivo contraction protocol. Reductions of key mitochondria-associated proteins occurred in both MA and IM muscles of ORC mice compared with CON, including PGC-1β, a homologue to PGC-1α with overlapping functions, and mitochondrial complex IV-associated proteins Cyt-C and COX-IV. These changes, which are consistent with loss of mitochondrial function, appear to be unrelated to biological age and are perhaps more dependent on the loss of testosterone production and/or IM/reduced function, again suggesting that these are early changes in progression towards sarcopenia and require attention after bed rest. Further investigation into the long-term functional consequences of this model is needed.

The MA animals showed characteristics consistent with early sarcopenia; thus, investigating this MA period could be more therapeutically modifiable than diagnosable sarcopenia. It is important to recognize that while we focused on the muscle-related issues with best rest and aging, there are a plethora of factors beyond muscle that have not been assessed. For example, the interaction between muscle and neural input, cognitive decline, the cardiovascular system, or bone morphology have not been characterized here. Our

approach produces complicated fibre-type-specific changes in fast-twitch (EDL) and slow-twitch (soleus) muscles, which could be translatable to many muscle-associated diseases. Furthermore, it is important to highlight that our combination model of IM and ORC may best represent the muscle changes associated with prolonged inactivity or acute bed rest seen in middle- and older-age individuals rather than aging or atrophy alone. As such, the model would be very useful for investigating ways to minimize the deleterious muscle effects of acute hospitalization or other acute atrophic conditions, such as casting or bed rest. Further, severity can easily be manipulated by altering the casting and castration time, the latter of which is relatively short compared with other works.[47]

One major limitation of this study worth noting is the exclusive use of male mice, and thus, we are unable to delineate and compare the results of the combined intervention with those of females. A recent study by de Jong et al. provided insights into the muscle response to the aging process in human biopsies, and it was found that indeed, males and females possess similar changes to varying molecular pathways in muscle, specifically in the mitochondria.[48] However, the magnitude of these changes is amplified in females, especially in the AMPK/Akt growth pathway, and the reasonings for this are not clearly defined. It is possible that depletion of androgens during menopause and/or the sex differences in muscle phenotype (i.e., females contain more type I fibres than males at a young age) may be driving the discrepancies observed in humans. Based on this, it is reasonable to suggest that if we were to mimic our current study in female mice, the overall phenotypic changes may not differ from age-matched CONs, but the molecular underpinnings will vary. The IM aspect included in our model, in addition to androgen depletion, introduces another level of complexity and requires further investigation, especially in female ovariectomized mice.

Therefore, the model can be used to investigate preventative measures to counteract the vast number of decrements displayed in this study. In addition, this model can also be used to explore pre-clinical interventions aimed at the rehabilitation phase (cast removal), which can be specifically related to recovery from acute hospitalization in humans.

In summary, while not a model of sarcopenia per se, we present baseline data from a modifiable pre-clinical mouse model that mimics the muscle-related changes seen in the peri-sarcopenia period. As such, the application of potential therapeutics, particularly during the rehabilitation phase in a low-testosterone environment, could be most valuable to temper the clinical trajectory of rapid aging. Therefore, we deem that our model could be a cost- and time-efficient tool for the pre-clinical testing of experimental therapeutics for the treatment of conditions where muscle loss and dysfunction are common features.

Acknowledgements

We thank the animal facilities staff at Victoria University for their expert animal care and support.

Open access publishing facilitated by Victoria University, as part of the Wiley - Victoria University agreement via the Council of Australian University Librarians.

Conflict of interest statement

The authors have no conflicts of interest to declare in relation to this study.

Funding

No formal funding was obtained. The work was supported through a Higher Degree by Research budget allocation from the Institute for Health and Sport, Victoria University.

Ethics statement

The authors of this manuscript certify that they comply with the ethical guidelines for authorship and publishing in the *Journal of Cachexia, Sarcopenia and Muscle*.[49]

Data availability statement

The data that support the findings of this study are available from the corresponding author upon reasonable request.

Online supplementary material

Additional supporting information may be found online in the Supporting Information section at the end of the article.

Table S1. Absolute muscle weights.
Figure S1. Organ and tissue weight of control (CON; black), middle-aged (MA; orange) and orchiectomised-immobilised (ORC; blue) mice.
Figure S2. Muscle twitch force characteristics of extensor digitorum longus (EDL) and soleus (SOL) muscles of control (CON), middle-aged (MA) and orchiectomised-immobilised (ORC) mice.
Figure S3. Haemotoxylin and eosin (H&E) staining for general muscle architecture of the extensor digitorum longus (EDL) and soleus (SOL) muscles.
Figure S4. Full-length Western blot images associated with Figure 5.

References

1. Sandonà D, Desaphy JF, Camerino GM, Bianchini E, Ciciliot S, Danieli-Betto D, et al. Adaptation of mouse skeletal muscle to long-term microgravity in the MDS mission. *PLoS ONE*. 2012;**7**:e33232.
2. Trevino MB, Zhang X, Standley RA, Wang M, Han X, Reis FCG, et al. Loss of mitochondrial energetics is associated with poor recovery of muscle function but not mass following disuse atrophy. *Am J Physiol Endocrinol Metab*. 2019;**317**:E899–E910.
3. Kalyani RR, Corriere M, Ferrucci L. Age-related and disease-related muscle loss: the effect of diabetes, obesity, and other diseases. *Lancet Diabet Endocrinol*. 2014; **2**:819–829.
4. Handelsman DJ, Sikaris K, Ly LP. Estimating age-specific trends in circulating testosterone and sex hormone-binding globulin in males and females across the lifespan. *Ann Clin Biochem*. 2016;**53**: 377–384.
5. Storer TW, Basaria S, Traustadottir T, Harman SM, Pencina K, Li Z, et al. Effects of testosterone supplementation for 3 years on muscle performance and physical function in older men. *J Clin Endocrinol Metab*. 2017;**102**:583–593.
6. Lynch GS. Identifying the challenges for successful pharmacotherapeutic management of sarcopenia. *Expert Opin Pharmacother.* 2022;**23**:1233–1237.
7. Cruz-Jentoft AJ, Bahat G, Bauer J, Boirie Y, Bruyère O, Cederholm T, et al. Sarcopenia: revised European consensus on definition and diagnosis. *Age Ageing*. 2018;**48**:16–31.
8. Fox JG, Davisson M, Newcomer CE, Quimby FW, Smith A. The mouse in aging research. In Fox JG, ed. *The mouse in biomedical research*, 2nd ed. Burlington, MA: American College Laboratory Animal Medicine (Elsevier); 2007. p 637–672.
9. Christian CJ, Benian GM. Animal models of sarcopenia. *Aging Cell*. 2020;**19**:e13223.
10. Wang S, Lai X, Deng Y, Song Y. Correlation between mouse age and human age in anti-tumor research: significance and method establishment. *Life Sci*. 2020; **242**:117242.
11. Percie du Sert N, Ahluwalia A, Alam S, Avey MT, Baker M, Browne WJ, et al. Reporting animal research: explanation and elaboration for the ARRIVE guidelines 2.0. *PLoS Biol*. 2020;**18**:e3000411.
12. Zhang H, Lin S, Chen X, Gu L, Zhu X, Zhang Y, et al. The effect of age, sex and strains on the performance and outcome in animal models of stroke. *Neurochem Int*. 2019;**127**:2–11.
13. Madaro LS, Molinaro P, Bouché M. Unilateral immobilization: a simple model of limb atrophy in mice. *Basic Appl Myol*. 2008;**18**: 149–153.
14. Kang C, Goodman CA, Hornberger TA, Ji LL. PGC-1α overexpression by in vivo transfection attenuates mitochondrial deterioration of skeletal muscle caused by immobilization. *FASEB J*. 2015;**29**: 4092–4106.
15. Debruin DA, Timpani CA, Lalunio H, Rybalka E, Goodman CA, Hayes A. Exercise may ameliorate the detrimental side effects of high vitamin D supplementation on muscle function in mice. *J Bone Miner Res*. 2020; **35**:1092–1106.
16. Brooks SV, Faulkner JA. Contractile properties of skeletal muscles from young, adult and aged mice. *J Physiol*. 1988;**404**:71–82.
17. Pal R, Palmieri M, Loehr JA, Li S, Abo-Zahrah R, Monroe TO, et al. Src-dependent impairment of autophagy by oxidative stress in a mouse model of Duchenne muscular dystrophy. *Nat Commun*. 2014; **5**:4425.
18. Davidyan A, Pathak S, Baar K, Bodine SC. Maintenance of muscle mass in adult male mice is independent of testosterone. *PLoS ONE*. 2021;**16**:e0240278.
19. Gaffney CJ, Pollard A, Barratt TF, Constantin-Teodosiu D, Greenhaff PL, Szewczyk NJ. Greater loss of mitochondrial function with ageing is associated with earlier onset of sarcopenia in *C. elegans*. *Aging (Albany NY)*. 2018;**10**:3382–3396.
20. Moore TM, Lin AJ, Strumwasser AR, Cory K, Whitney K, Ho T, et al. Mitochondrial dysfunction is an early consequence of partial or complete dystrophin loss in mdx mice. *Front Physiol*. 2020;**11**:690.
21. Hanson ED, Betik AC, Timpani CA, Tarle J, Zhang X, Hayes A. Testosterone suppression does not exacerbate disuse atrophy and impairs muscle recovery that is not rescued by high protein. *J Appl Physiol*. 2020;**129**:5–16.
22. Mirosevich J, Bentel JM, Zeps N, Redmond SL, D'Antuono MF, Dawkins HJ. Androgen receptor expression of proliferating basal and luminal cells in adult murine ventral prostate. *J Endocrinol*. 1999;**162**:341–350.
23. Delmonico MJ, Harris TB, Visser M, Park SW, Conroy MB, Velasquez-Mieyer P, et al. Longitudinal study of muscle strength, quality, and adipose tissue infiltration. *Am J Clin Nutr.* 2009;**90**:1579–1585.
24. Morrison S, Colberg SR, Parson HK, Neumann S, Handel R, Vinik EJ, et al. Walking-induced fatigue leads to increased falls risk in older adults. *J Am Med Dir Assoc*. 2016;**17**:402–409.
25. Addison O, Drummond MJ, Lastayo PC, Dibble LE, Wende AR, McClain DA, et al. Intramuscular fat and inflammation differ in older adults: the impact of frailty and inactivity. *J Nutr Health Aging*. 2014;**18**: 532–538.
26. Gonzalez-Freire M, Scalzo P, D'Agostino J, Moore ZA, Diaz-Ruiz A, Fabbri E, et al. Skeletal muscle ex vivo mitochondrial respiration parallels decline in vivo oxidative capacity, cardiorespiratory fitness, and muscle strength: the Baltimore Longitudinal Study of Aging. *Aging Cell*. 2018; **17**:17(2).
27. Marzetti E, Calvani R, Cesari M, Buford TW, Lorenzi M, Behnke BJ, et al. Mitochondrial dysfunction and sarcopenia of aging: from signaling pathways to clinical trials. *Int J Biochem Cell Biol*. 2013;**45**: 2288–2301.
28. Pietrangelo L, D'Incecco A, Ainbinder A, Michelucci A, Kern H, Dirksen RT, et al. Age-dependent uncoupling of mitochondria from Ca^{2+} release units in skeletal muscle. *Oncotarget*. 2015;**6**:35358–35371.
29. Del Campo A, Contreras-Hernández I, Castro-Sepúlveda M, Campos CA, Figueroa R, Tevy MF, et al. Muscle function decline and mitochondria changes in middle age precede sarcopenia in mice. *Aging*. 2018; **10**:34–55.
30. Timpani CA, Hayes A, Rybalka E. Revisiting the dystrophin-ATP connection: how half a century of research still implicates mitochondrial dysfunction in Duchenne Muscular Dystrophy aetiology. *Med Hypotheses*. 2015;**85**:1021–1033.
31. Campelj DG, Timpani CA, Petersen AC, Hayes A, Goodman CA, Rybalka E. The paradoxical effect of PARP inhibitor BGP-15 on irinotecan-induced cachexia and skeletal muscle dysfunction. *Cancers (Basel)*. 2020; **12**:12.
32. Hughes DC, Marcotte GR, Marshall AG, West DWD, Baehr LM, Wallace MA, et al. Age-related differences in dystrophin: impact on force transfer proteins, membrane integrity, and neuromuscular junction stability. *J Gerontol A Biol Sci Med Sci*. 2017; **72**:640–648.
33. Janssen I, Heymsfield SB, Wang ZM, Ross R. Skeletal muscle mass and distribution in 468 men and women aged 18–88 yr. *J Appl Physiol*. 2000;**89**:81–88.
34. Bickle SC, Cross JM, Bamman MM. Exercise dosing to retain resistance training adaptations in young and older adults. *Med Sci Sports Exerc*. 2011;**43**:1177–1187.
35. Lin X, Hanson E, Betik AC, Brennan-Speranza TC, Hayes A, Levinger I. Hindlimb immobilization, but not castration, induces reduction of undercarboxylated osteocalcin associated with muscle atrophy in rats. *J Bone Miner Res*. 2016;**31**:1967–1978.
36. McPhee JS, Cameron J, Maden-Wilkinson T, Piasecki M, Yap MH, Jones DA, et al. The contributions of fiber atrophy, fiber loss, in situ specific force, and voluntary activation to weakness in sarcopenia. *J Gerontol: Series A*. 2018;**73**:1287–1294.
37. Summers TB, Hines HM. Effect of immobilization in various positions upon the weight and strength of skeletal muscle. *Arch Phys Med Rehabil*. 1951;**32**:142–145.
38. Spector SA, Simard CP, Fournier M, Sternlicht E, Edgerton VR. Architectural alterations of rat hind-limb skeletal muscles immobilized at different lengths. *Exp Neurol*. 1982;**76**:94–110.
39. Distefano G, Standley RA, Zhang X, Carnero EA, Yi F, Cornnell HH, et al. Physical activity

unveils the relationship between mitochondrial energetics, muscle quality, and physical function in older adults. *J Cachexia Sarcopenia Muscle*. 2018;**9**:279–294.
40. Larsson L, Degens H, Li M, Salviati L, Lee Y, Thompson W, et al. Sarcopenia: aging-related loss of muscle mass and function. *Physiol Rev*. 2019;**99**:427–511.
41. Coen PM, Musci RV, Hinkley JM, Miller BF. Mitochondria as a target for mitigating sarcopenia. *Front Physiol*. 2019;**9**:1883.
42. Chabi B, Ljubicic V, Menzies KJ, Huang JH, Saleem A, Hood DA. Mitochondrial function and apoptotic susceptibility in aging skeletal muscle. *Aging Cell*. 2008;**7**:2–12.
43. Wanagat J, Cao Z, Pathare P, Aiken JM. Mitochondrial DNA deletion mutations colocalize with segmental electron transport system abnormalities, muscle fiber atrophy, fiber splitting, and oxidative damage in sarcopenia. *FASEB J*. 2001;**15**: 322–332.
44. Kruse SE, Karunadharma PP, Basisty N, Johnson R, Beyer RP, MacCoss MJ, et al. Age modifies respiratory complex I and protein homeostasis in a muscle type-specific manner. *Aging Cell*. 2016;**15**: 89–99.
45. Herbst A, Pak JW, McKenzie D, Bua E, Bassiouni M, Aiken JM. Accumulation of mitochondrial DNA deletion mutations in aged muscle fibers: evidence for a causal role in muscle fiber loss. *J Gerontol A Biol Sci Med Sci*. 2007;**62**:235–245.
46. Guillot C, Steinberg JG, Delliaux S, Kipson N, Jammes Y, Badier M. Physiological, histological and biochemical properties of rat skeletal muscles in response to hindlimb suspension. *J Electromyogr Kinesiol*. 2008; **18**:276–283.
47. Rossetti ML, Dunlap KR, Salazar G, Hickner RC, Kim JS, Chase BP, et al. Systemic delivery of a mitochondria targeted antioxidant partially preserves limb muscle mass and grip strength in response to androgen deprivation. *Mol Cell Endocrinol*. 2021; **535**:111391.
48. de Jong J, Attema BJ, van der Hoek MD, Verschuren L, Caspers MPM, Kleemann R, et al. Sex differences in skeletal muscle-aging trajectory: same processes, but with a different ranking. *Geroscience*. 2023;**45**:2367–2386.
49. von Haehling S, Coats AJS, Anker SD. Ethical guidelines for publishing in the Journal of Cachexia, Sarcopenia and Muscle: Update 2023. *J Cachexia Sarcopenia Muscle*. 2023;**14**:2981–2983.